Effects of co-doping in semiconductors: CdTe

Baoying Dou, Qingde Sun, and Su-Hai Wei*
Beijing Computational Science Research Center, Beijing 100193, China

(Received 22 September 2021; accepted 19 November 2021; published 7 December 2021)

Co-doping is an important method to improve doping properties in semiconductors, which is expected to lower the defect formation energy through the Coulomb interaction or covalent coupling between co-dopants and reduce the transition energy level through the level repulsions. However, the effectiveness of co-doping is sensitive to the type of co-dopants, and in some cases, negative effects can exist. Here, using *p*-type doping in CdTe as an example, we systematically investigate different dopant combinations based on first-principles hybrid functional calculations. We show that the complex of one donor + one double acceptor, e.g., $Cl_{Te} + V_{Cd}$, can cause a decrease in defect formation energy and a reduction in acceptor level, thus improving the dopability, especially when the Cl treatment is done at low temperature. The combination of two acceptors + one donor, e.g., $Cl_{Te} + 2Cu_{Cd}$, has little or even negative effects because of the coexistence of the acceptor-acceptor and donor-acceptor coupling. More importantly, we show that the combination of one deep acceptor + one shallow acceptor, e.g., $Sb_{Te} + P_{Te}$, produces a much deeper acceptor level because the nominal deep acceptor Sb_{Te} acts as a donor with respect to the shallow one, and then the deep acceptor state will be pushed even deeper due to the level repulsion. Thus, we should avoid this type of acceptor-acceptor co-doping to achieve high hole concentration. Our general understanding of the co-doping approach, therefore, provides a guideline for the future design of shallow defect complexes in CdTe and other semiconductors.

DOI: 10.1103/PhysRevB.104.245202

I. INTRODUCTION

Co-doping is a promising strategy to enhance the dopability by lowering the defect formation energy and ionization energy level through the coupling of the dopants [1,2], which has been successfully applied to some wide-gap semiconductors. For example, because the wave function of V_{Zn} is mostly localized on the neighboring O atoms in ZnO, the co-doping of more electronegative F substitution on the O site forming $V_{Zn} + F_O$ could pull down the V_{Zn} level, thus making the acceptor level shallower. In CdTe, previous theoretical calculations based on the local density approximation show that the defect complex composed of a single donor and a double acceptor such as $V_{Cd} + Cl_{Te}$ helps to improve *p*-type doping in CdTe [3]. However, the co-doping strategy does not always work. Some studies have shown that donor-acceptor defect complexes have no or even negative effects on decreasing the formation and ionization energies [4]. For example, Cu is often used as a *p*-type dopant in CdTe because Cu_{Cd} is relatively easily ionized [5,6]. Considering that Cu_{Cd} is a single acceptor, two of them are needed to combine with the single donor Cl_{Te} to form an acceptor complex $2Cu_{Cd} + Cl_{Te}$. However, it is not guaranteed that such a complex (two acceptors + one donor) is effective on *p*-type doping due to the coupling between the two acceptors.

CdTe is one of the most promising absorber materials in thin film solar cells due to its direct bandgap of ~1.5 eV and large optical absorption coefficient [7]. Specifically, CdTe is the only II-VI semiconductor that can relatively easily achieve both *p*- and *n*-type doping [8], making it an attractive material in optoelectronic device applications [9,10]. However, efficient *p*-type doping has been a challenge for CdTe due to the high transition energy levels and self-compensation of its intrinsic defects. Great efforts have been made so far to increase its hole carrier density and power conversion efficiency, but the solar cell efficiency has reached only to 22.1% [11], which is still much lower than the maximum theoretical efficiency (~32%). In CdTe, typically, the samples are grown under Cd-poor conditions to facilitate the formation of V_{Cd} or Cu_{Cd}, but recent theoretical and experimental studies [12,13] show that, under Cd-poor conditions, some detrimental defects such as Te on Cd antisites Te_{Cd} are also easy to form, which have been identified as the main nonradiative recombination centers in CdTe. Therefore, it has been proposed that group-V (P, As, and Sb) substitution on Te sites under Cd-rich conditions should be a more effective approach [14–19]. Thus, here, we will test to see if the complex $2X_{Te} + Cl_{Te}$ (X = P, As, Sb) can also be as effective as $V_{Cd} + Cl_{Te}$ in reducing the transition energy levels. Moreover, acceptor Sb_{Te} has a relatively deep transition energy level due to its high *p* orbital energy [18,20,21], whereas acceptor P_{Te} has a shallow transition energy level. One may think that, if we co-dope CdTe with both P_{Te} and Sb_{Te}, the hole carrier concentration could add up so that the hole carrier density would increase compared with that if only one type of acceptor is doped. However, we will show that such a concept of mixed doping is misleading, and this type of acceptor-acceptor co-doping should be avoided.

In this paper, the three kinds of co-doping combinations in CdTe, as discussed above, are studied using first-principles

*suhuaiwei@csrc.ac.cn

 ©2021 American Physical Society

hybrid functional calculations. We discuss the general trends and the underlying mechanisms behind them. Our calculations show that only the combination of one double acceptor + one donor has beneficial effects on *p*-type doping in reducing the acceptor formation energy due to the charge transfer from donor to acceptor and subsequent Coulomb interaction between the co-dopants and in reducing the ionization energy through the level repulsion due to the reduced symmetry of the defect pairs. The combination of two acceptors + one donor has small or even negative effects on dopability due to the coexistence of the acceptor-acceptor and donor-acceptor coupling. The combination of one deep acceptor + one shallow acceptor will in general lead to a defect transition energy level even deeper than the deep one unless the deep acceptor is not occupied because the deep acceptor acts as a donor compared with the shallow one if the deep level is partially occupied by electrons. Our results show that, in general, the mixed acceptor-acceptor co-doping should be avoided to keep the shallowness of the acceptor level. Our general understanding of the co-doping, therefore, provides critical insight for designing useful defect complexes to achieve better *p*-type doping in CdTe and can be used as a guideline for co-doping in other semiconductors.

II. METHODS OF CALCULATION

First-principles calculations were performed using density functional theory [22] with the frozen-core projector augmented wave approach [23] as implemented in the VASP code [24]. The Heyd-Scuseria-Ernzerhof 2006 (HSE06) hybrid functional [25] with $\alpha = 0.25$ was employed because it could reproduce the correct lattice constant and bandgap of semiconductors [26]. The valence electron configurations were Cd($4d^{10}5s^2$), Te($5s^25p^4$), Cl($3s^23p^5$), group-V(s^2p^3), and Cu($3p^63d^{10}4s^1$), respectively, where the Cu $3p$ orbital is considered as a semicore state for better description. All calculations adopted a cutoff energy of 350 eV, except for Cu-related calculations with cutoff energy of 400 eV. Our calculated lattice constant and bandgap for pure CdTe were 6.56 Å and 1.52 eV, respectively, in good agreement with the experimental values of 6.48 Å and 1.56 eV [27]. For the defect calculations, a 216-atom zinc blende supercell was constructed, and we used only the Γ-point for k-point sampling [28]. The lattice constants of supercells were fixed to that of pure CdTe, and all the atoms in the supercells were fully relaxed until the Hellmann-Feynman force on every atom was <0.05 eV/Å.

The defect formation energy is a function of the electron Fermi energy E_F and the atomic chemical potentials μ_i, which is determined by [28]

$$\Delta H_f(\alpha, q) = \Delta E(\alpha, q) + \sum_i n_i\mu_i + qE_F, \tag{1}$$

where $\Delta E(\alpha, q) = E(\alpha, q) - E(\text{host}) + \sum_i n_iE_i + qE_{\text{VBM}}$. Here, $E(\alpha, q)$ is the total energy of a supercell with a defect α in charge state q, and $E(\text{host})$ is the total energy of the same supercell without defect. Here, n_i is the number of atoms, and q is the number of electrons transferred from the supercell to the reservoirs in forming the defect cell. Here, E_i is the total energy of elemental solid or gas, and μ_i is the chemical potential of constituent i with respect to E_i. Here, E_F is referenced to E_{VBM}(host), i.e., the valence band maximum (VBM) of the host. The eigenvalues of the defect-containing and defect-free cells are aligned using the core level of the atom away from the defect. The defect transition energy level $\epsilon_\alpha(q/q')$ is the Fermi energy in Eq. (1) at which the defect α has the same formation energy in two different charge states q and q':

$$\epsilon_\alpha(q/q') = \frac{\Delta E(\alpha, q) - \Delta E(\alpha, q')}{q' - q}. \tag{2}$$

A 512-atom supercell was used to test the convergence, and we found that the defect transition energy levels were well converged to within 0.1 eV.

Under equilibrium growth conditions, the chemical potentials μ_i in Eq. (1) are limited by several conditions. Consider, for example, the case of CdTe: $2X_{\text{Te}} + \text{Cl}_{\text{Te}}$ (X = P, As, Sb). Firstly, to avoid the precipitation of elemental dopants and host elements, we should have

$$\mu_i \leqslant 0. \tag{3}$$

Secondly, the stable CdTe compound should be maintained, thus,

$$\mu_{\text{Cd}} + \mu_{\text{Te}} = \Delta H_f(\text{CdTe}), \tag{4}$$

where $\Delta H_f(\text{CdTe})$ is the formation energy of bulk CdTe, and the calculated value is -1.16 eV, consistent with the previous HSE06 results [6,29] and close to the experimental value of -0.96 eV [30]. Finally, to avoid the formation of the possible secondary phases between the dopants and host elements, μ_i are bound by

$$\mu_{\text{Cd}} + 2\mu_{\text{Cl}} \leqslant \Delta H_f(\text{CdCl}_2), \tag{5}$$

$$m\mu_{\text{Cd}} + n\mu_X \leqslant \Delta H_f(\text{Cd}_mX_n). \tag{6}$$

The calculated formation energy of $CdCl_2$ is -3.61 eV, in good agreement with previous calculations [21,29,31]. Here, Cd_3P_2, Cd_3As_2, and Cd_3Sb_2 were taken as the limiting secondary phases because they are the most stable ones in Cd_mP_n, Cd_mAs_n, and Cd_mSb_n compounds [32,33]. The calculated formation energies of Cd_3P_2, Cd_3As_2, and Cd_3Sb_2 are -0.60, -0.82, and -0.37 eV, respectively.

To determine whether the defect pair (e.g., $2X_{\text{Te}} + \text{Cl}_{\text{Te}}$) is stable, the binding energy is defined as

$$E_b^q(E_F) = \Delta H^q_{f,\text{complex}}(E_F) - \sum_i \Delta H^{q_i}_{f,\text{defect(i)}}(E_F) + \left(q - \sum_i q_i\right)E_F, \tag{7}$$

where $\Delta H^q_{f,\text{complex}}(E_F)$ and $\Delta H^{q_i}_{f,\text{defect(i)}}(E_F)$ are the formation energies of the complex and isolated defects, respectively, in their most stable charge state q and q_i, respectively, given the Fermi energy E_F. Generally, in a wide range of the Fermi energy, the charges of the isolated defects add up to the charge of the complex, so the binding energy is a constant. Otherwise, the binding energy could depend on the Fermi energy. Negative binding energy indicates that the defect complexes

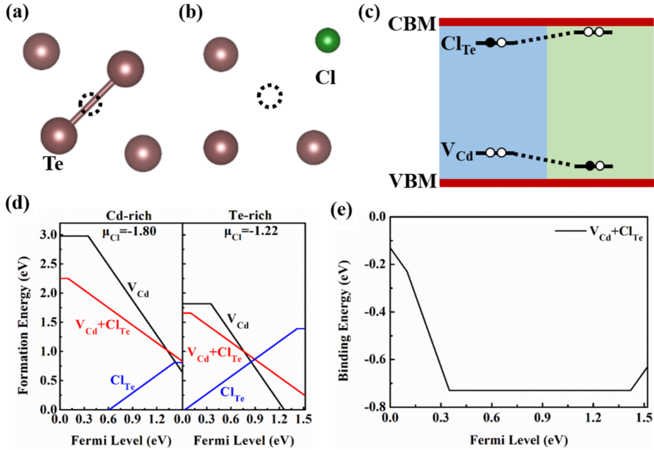

FIG. 1. (a) and (b) Local atomic structures for V_{Cd} and $V_{Cd} + Cl_{Te}$, respectively, where the brown sphere represents Te, the green one represents Cl, and the black dash-dotted circle represents the Cd vacancy. (c) Schematic diagram to show the effects of co-doping on defect transition energy levels in the formation of $V_{Cd} + Cl_{Te}$. The first and second columns exhibit the transition levels before and after the donor-acceptor coupling, respectively. (d) Calculated defect formation energies of $V_{Cd} + Cl_{Te}$ and the corresponding individual defects, as functions of the Fermi levels, under Cd- and Te-rich conditions, where the slope of formation energy gives the charge state of the defect, and the turning point gives the defect transition energy level. Here, the chemical potentials are bound by $\mu_{Cd} + \mu_{Te} = -1.16$ eV and $\mu_{Cd} + 2\mu_{Cl} < -3.61$ eV. (e) Calculated binding energy of the complex $V_{Cd} + Cl_{Te}$ as a function of the Fermi level.

tend to bind with each other when both are present in the system.

III. RESULTS AND DISCUSSIONS

A. One double acceptor + one donor

Figure 1(a) plots the defect structure of V_{Cd} after relaxation, where the large local Jahn-Teller distortion happens: two Te atoms neighboring a Cd vacancy move toward each other, and the other two Te atoms move away from each other, thus splitting the original threefold degenerate state into a twofold degenerate fully occupied state below the VBM and an empty state above it. Our total energy calculation shows that V_{Cd} has a negative-U behavior, i.e., the neutral defect prefers to accept two electrons from the VBM rather than one electron, which is caused by the large local atomic relaxation around the neutral defect. Thus, the (0/−2) transition energy level of V_{Cd} is relatively deep due to the large atomic relaxation, ~0.35 eV above the VBM, as shown in Fig. 1(d), in good agreement with previous HSE06 calculations [12,34].

To lower the defect transition level, Cl is usually co-doped in CdTe to form the defect complex $V_{Cd} + Cl_{Te}$ (A center), which consists of one double acceptor and one single donor. The structure of the A center is shown in Fig. 1(b), where Cl moves toward its three Cd neighbors, i.e., away from the Cd vacancy site to form stronger Cl-Cd bonds. Our calculation of $V_{Cd} + Cl_{Te}$ is compared with that of $V_{Cd} + I_{Te}$, which confirms that the displacement of the Cl is mainly due to its small size compared with Te. The calculated defect formation energies and transition energy levels are shown in Fig. 1(d), where the A center has a (0/−) transition level of 0.10 eV above the VBM, much shallower than that of V_{Cd}, which agrees well with previous theoretical studies [6,31,35]. This can be understood as follows. As shown in Fig. 1(c), to form the A center, the donor Cl_{Te} donates one electron to its nearest neighbor V_{Cd} which serves as an acceptor, and then the symmetry-reduction-induced coupling between them pushes the acceptor level down and the donor level up, thus greatly reducing the acceptor ionization energy. The calculated binding energy of the A center is shown in Fig. 1(e), which indicates that the complex $V_{Cd} + Cl_{Te}$ is stable within the entire Fermi level region inside the bandgap. This large binding energy results from the energy gain caused by charge transfer from Cl_{Te} to V_{Cd} and the strong Coulomb attraction between the positively charged Cl donor and negatively charged V_{Cd} acceptor. The A center has a much shallower acceptor level and a lower formation energy than V_{Cd}. This is consistent with the experimental observations that Cl treatment helps to improve *p*-type doping in CdTe [10,36,37]. However, it should be noted that the amount of Cl needs to be controlled because too much Cl will overcompensate the complex and turn the system into *n* type [6,35,38,39].

B. Two acceptors + one donor

For Cu and Cl co-doping in CdTe to form a *p*-type complex, two Cu atoms and one Cl atom are combined to form the acceptor $2Cu_{Cd} + Cl_{Te}$ because Cu and Cl are single acceptor and single donor, respectively. Considering the repulsion between acceptors and the attraction between acceptor and donor, to lower the Coulomb energy of the complex, the two Cu atoms should be close to the Cl atom but far apart from each other, as shown in Fig. 2(b). Figure 2(d) displays the calculated binding energy of $2Cu_{Cd} + Cl_{Te}$, indicating that it is stable within the entire Fermi level region. Compared with the complex $V_{Cd} + Cl_{Te}$, the binding of $2Cu_{Cd} + Cl_{Te}$ is weak in general due to the repulsion between the two Cu_{Cd}. We calculate the (0/−) transition energy level of the complex and find that it is 0.11 eV above the VBM compared with Cu_{Cd} of 0.08 eV above the VBM, but the defect formation energy is significantly higher than that of Cu_{Cd}, as seen in Fig. 2(c). Therefore, Cl co-doping with Cu shows only little help on the improvement of *p*-type doping [3,21].

For the complex $2X_{Te} + Cl_{Te}$ ($X =$ P, As, Sb), it is plausible that the structure $(2X_{Te} + Cl_{Te})$-II shown in Fig. 3(c) is more stable, where the two group-V atoms are more separated, leading to lower Coulomb repulsion energy than the structure $(2X_{Te} + Cl_{Te})$-I shown in Fig. 3(b). Our calculations show that it is indeed the case for $2P_{Te} + Cl_{Te}$ and $2As_{Te} + Cl_{Te}$ but not for $2Sb_{Te} + Cl_{Te}$. The calculated transition energy levels and formation energies for relevant defects are listed in Table I. As we can see, the structure shown in Fig. 3(b) is more stable for $2Sb_{Te} + Cl_{Te}$, with a deeper acceptor level than the structure in Fig. 3(c). This can be understood as follows. Note that the difference between the structures in Figs. 3(b) and 3(c) is the Sb-Sb distance. Figure 3(b) suggests that it has stronger coupling between the two Sb atoms. To confirm this idea, we performed the defect calculations of $2Sb_{Te}$ with two

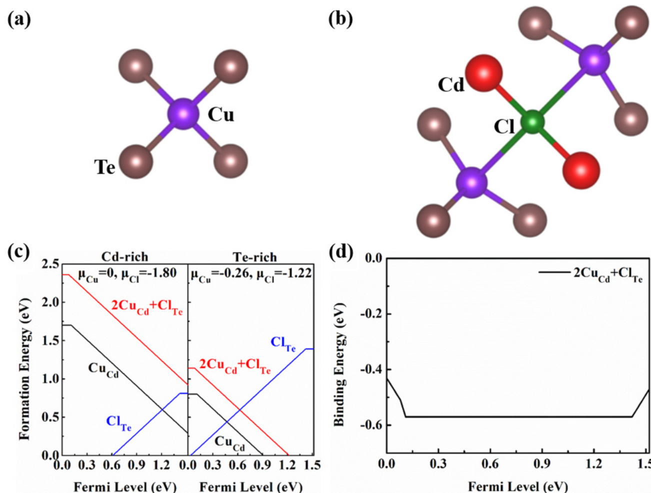

FIG. 2. (a) and (b) Local atomic structures for Cu_{Cd} and $2Cu_{Cd} + Cl_{Te}$, respectively. (c) Calculated defect formation energies of $2Cu_{Cd} + Cl_{Te}$ and the corresponding individual defects, as functions of the Fermi levels, under Cd- and Te-rich conditions. Here, the chemical potentials are bound by $\mu_{Cd} + \mu_{Te} = -1.16$ eV, $\mu_{Cu} + \mu_{Te} < -0.26$ eV, and $\mu_{Cd} + 2\mu_{Cl} < -3.61$ eV. (d) Calculated binding energy of the complex $2Cu_{Cd} + Cl_{Te}$ as a function of the Fermi level.

structures $(2Sb_{Te})$-I and $(2Sb_{Te})$-II and compared them with that of $2P_{Te}$. Our results show that $(2Sb_{Te})$-I has a (0/2−) transition level of 0.61 eV above the VBM, much deeper than that of 0.30 eV above the VBM for $(2Sb_{Te})$-II, which indicates that the strong coupling between the two Sb defect states in the structure of $(2Sb_{Te})$-I leads to a large energy gain, as shown in Fig. 4(a). Thus, $(2Sb_{Te})$-I is more stable than $(2Sb_{Te})$-II, like the case of $2Sb_{Te} + Cl_{Te}$. Our calculations show that the neutral $(2Sb_{Te})$-I is 0.09 eV lower in energy than the neutral $(2Sb_{Te})$-II, but the 2− charged $(2Sb_{Te})$-I is 0.12 eV higher in energy than the 2− charged $(2Sb_{Te})$-II. This is because the defect state of $2Sb_{Te}$ in the 2− charged state is fully occupied; therefore, there is no energy gain due to the covalent coupling, as seen in Fig. 4(b). In this case, the Coulomb repulsion energy between the negatively charged Sb_{Te}^{-} leads to the higher energy of the 2− charged $(2Sb_{Te})$-I than the 2− charged $(2Sb_{Te})$-II. The case of $2Sb_{Te} + Cl_{Te}$ is like that of $2Sb_{Te}$. As for P-doped complexes, because the localized orbital of the P element leads to weak acceptor-acceptor coupling and small energy gain, the Coulomb repulsion between the two negatively charged acceptors is dominant, which makes the two P atoms tend to move away from each other. Figure 5(a) plots the calculated defect formation energies for group-V doped defect complexes and individual defects. It shows that, for the

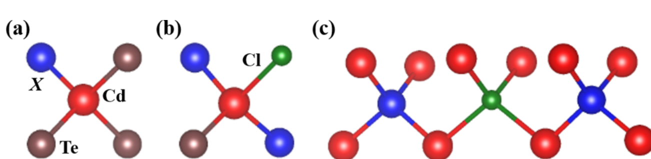

FIG. 3. Local atomic structures for (a) X_{Te}, (b) $(2X_{Te} + Cl_{Te})$-I, and (c) $(2X_{Te} + Cl_{Te})$-II, where X = P, As, Sb.

TABLE I. Calculated defect transition energy levels $\varepsilon(0/-)$ and formation energies of neutral defects under Cd-rich condition ΔH(Cd-rich) and under Te-rich condition ΔH(Te-rich) for group-V (X = P, As, Sb) individual defects X_{Te} and defect complexes with the structures $(2X_{Te} + Cl_{Te})$-I and $(2X_{Te} + Cl_{Te})$-II, respectively. All the energies are in electronvolts.

Defect	$\varepsilon(0/-)$	ΔH(Cd-rich)	ΔH(Te-rich)
P_{Te}	0.070	1.32	2.18
$(2P_{Te} + Cl_{Te})$-I	0.053	1.72	4.03
$(2P_{Te} + Cl_{Te})$-II	0.044	1.64	3.95
As_{Te}	0.079	1.27	2.02
$(2As_{Te} + Cl_{Te})$-I	0.100	1.63	3.71
$(2As_{Te} + Cl_{Te})$-II	0.069	1.57	3.65
Sb_{Te}	0.149	1.18	2.15
$(2Sb_{Te} + Cl_{Te})$-I	0.342	1.38	3.91
$(2Sb_{Te} + Cl_{Te})$-II	0.144	1.47	4.01

complexes $2P_{Te} + Cl_{Te}$ and $2As_{Te} + Cl_{Te}$, the acceptor levels are shallower than P_{Te} and As_{Te}, respectively, but the defect formation energies are larger with respect to the corresponding isolated defects. For the complex $2Sb_{Te} + Cl_{Te}$, it has a much deeper acceptor level and a higher formation energy than Sb_{Te}. Figure 5(b) shows the calculated binding energies of the complex $2X_{Te} + Cl_{Te}$ (X = P, As, Sb), which indicate that they are stable within the entire Fermi level region.

In general, our results show that the co-doping composed of two acceptors and one donor has little and even adverse effects on improving the doping effectiveness of the acceptors. This is because the acceptor-acceptor coupling pushes the acceptor level up, although the acceptor-donor coupling pushes the acceptor level down, as shown in Fig. 5(c). For group-V and Cl co-doping, the acceptor level cannot be significantly pulled down due to the large spatial distance and thus weak acceptor-donor coupling. Furthermore, forming extra point defects costs more energy, which is not adequately compensated by the Coulomb interaction between co-dopants, thus leading to an increase in the formation energy with respect to the isolated defects.

C. One deep acceptor + one shallow acceptor

Finally, we study the effect of one deep acceptor plus one shallow acceptor co-doping. Due to the similarity in size between Sb and Te, Sb substitution on Te in CdTe has a relatively low defect formation energy with respect to other group-V atoms, but it also has a rather deep defect level due to its high $5p$ orbital energy [18,20,21]. One may think, if we co-dope a

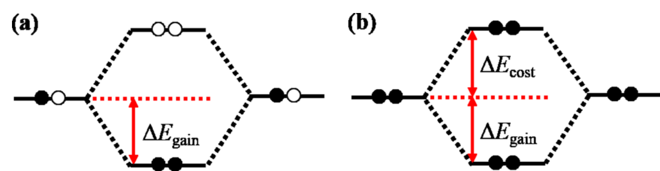

FIG. 4. Schematic diagram to show the coupling mechanism for two group-V dopants (a) in the neutral state and (b) in the charged state.

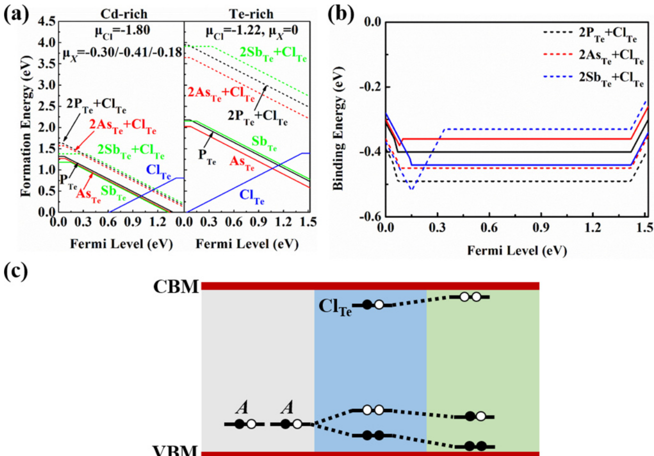

FIG. 5. (a) Calculated defect formation energies of $2X_{Cd} + Cl_{Te}$ ($X =$ P, As, Sb) and the corresponding individual defects as functions of the Fermi levels under Cd- and Te-rich conditions. (b) Calculated binding energies of the complex $2X_{Te} + Cl_{Te}$ ($X =$ P, As, Sb) as a function of the Fermi level. (c) Schematic diagram to show the effects of co-doping on defect transition energy levels in the formation of $2A + Cl_{Te}$, where A is the acceptor substituting on Cd or Te atoms. The first column exhibits the acceptor levels without coupling, the second column exhibits the acceptor levels with the acceptor-acceptor coupling but without the donor-acceptor coupling, and the third column exhibits the acceptor levels with the acceptor-acceptor and donor-acceptor coupling.

shallow acceptor (e.g., P_{Te}) with another acceptor Sb_{Te}, the total hole concentration may increase due to the combined effect. To check this idea, we construct the supercell with one Sb atom and one neighboring P atom substituting on the Te atom sites, as shown Fig. 6(a). From Fig. 6(d), the calculated binding energy is negative (binding) only when the Fermi energy is close to the VBM due to the increase of the formation energy of charged defects P_{Te} and Sb_{Te} near the VBM. The calculated acceptor level is 0.31 eV above the VBM, much deeper than that of Sb_{Te} of 0.15 eV above the VBM, as seen in Fig. 6(c). This is because the deep acceptor Sb_{Te} is acting as a donor with respect to the shallow acceptor P_{Te}. As shown in Fig. 6(b), Sb_{Te} donates one electron to P_{Te} and makes the shallow state fully occupied and the deep state unoccupied. Due to the level repulsion, the unoccupied state will be pushed up, and the occupied state will be pushed down. Thus, the final acceptor level is deeper than the isolated defects.

D. Solid solubility limit

In the following, we will discuss under what conditions the defect complexes can form. In the dilute doping limit, the defect concentration is given by

$$N(D) = N_{site} g_D \exp\left[-\frac{\Delta H(D)}{k_B T}\right], \tag{8}$$

where $N(D)$ is the number of defects D, N_{site} is the number of available sites per volume that may be occupied by the defect, g_D is the degeneracy factor per site, $\Delta H(D)$ is the formation energy, and T is the growth temperature. Taking the double-acceptor + single-donor co-doping case, i.e., $V_{Cd} + Cl_{Te}$ co-

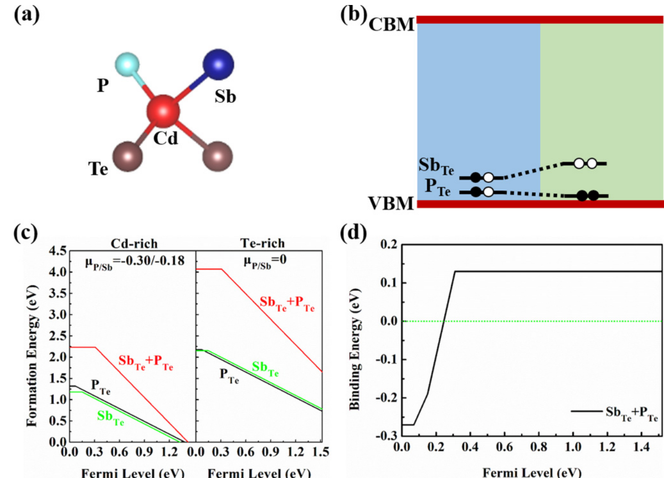

FIG. 6. (a) Local atomic structures for $Sb_{Te} + P_{Te}$. (b) Schematic diagram to show the effects of co-doping on defect transition energy levels in the formation of $Sb_{Te} + P_{Te}$. The first and second columns exhibit the transition levels before and after the acceptor-acceptor coupling, respectively. The inset shows the local atomic structures of $Sb_{Te} + P_{Te}$. (c) Calculated defect formation energies of $Sb_{Te} + P_{Te}$ and the corresponding individual defects as functions of the Fermi levels under Cd- and Te-rich conditions. (d) Calculated binding energies of the complex $Sb_{Te} + P_{Te}$ as a function of the Fermi level.

doping as an example, the concentrations of V_{Cd}, Cl_{Te}, and $V_{Cd} + Cl_{Te}$ are given by

$$N(V_{Cd}) = N_{site} \exp\left[-\frac{\Delta H(V_{Cd})}{k_B T}\right],$$
$$N(Cl_{Te}) = N_{site} \exp\left[-\frac{\Delta H(Cl_{Te})}{k_B T}\right],$$
$$N(V_{Cd} + Cl_{Te}) = 4N_{site} \exp\left[-\frac{\Delta H(V_{Cd} + Cl_{Te})}{k_B T}\right], \tag{9}$$

where the prefactors 1, 1, and 4 consider the site degeneracy. The total number of Cl atoms in the system is, thus, given by

$$N_{Cl}^{tot} = N(Cl_{Te}) + N(V_{Cd} + Cl_{Te}). \tag{10}$$

We can rewrite Eq. (9) as

$$[N(V_{Cd} + Cl_{Te})/N(Cl_{Te})] = 4[N(V_{Cd})/N_{site}] \exp\left(-\frac{E_b}{k_B T}\right), \tag{11}$$

where $E_b = \Delta H(V_{Cd} + Cl_{Te}) - \Delta H(V_{Cd}) - \Delta H(Cl_{Te})$ is the binding energy of the defect pair and has been calculated in Fig. 1(e). Note that Cl_{Te} is a donor; therefore, to have an effective p-type doping, the ratio of $[N(V_{Cd} + Cl_{Te})/N(Cl_{Te})]$ should be > 1, i.e., we need to have high defect concentration $N(V_{Cd})/N_{site}$ and high (negative) binding energy E_b and/or low Cl treatment temperature.

Assuming $N(V_{Cd})/N_{site}$ is $\sim 10^{-6}$ and the Cl treatment temperature is at 600 K, the calculated ratio of $[N(V_{Cd} + Cl_{Te})/N(Cl_{Te})]$ over the corresponding binding energy range is shown in Fig. 7. We can see that the ratio becomes >1 as the magnitude of the binding energy becomes larger than 0.65 eV. It means that, under realistic growth con-

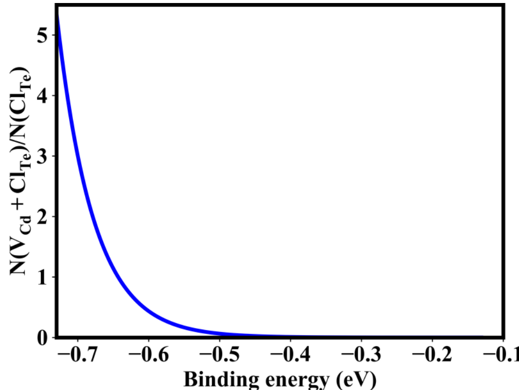

FIG. 7. The calculated ratio of $N(V_{Cd} + Cl_{Te})/N(Cl_{Te})$ over the corresponding binding energy range, assuming $N(V_{Cd})/N_{site}$ is $\sim 10^{-6}$, and the Cl treatment temperature is at 600 K.

ditions, it is possible to use Cl treatment to enhance p-type doping in CdTe by forming the $V_{Cd} + Cl_{Te}$ (A center) complex if there are enough Cd vacancies in the sample and the Cl treatment temperature is relatively low.

IV. CONCLUSIONS

In conclusion, the effectiveness of the co-doping concepts in semiconductors is carefully investigated. Taking p-type doping in CdTe as an example, based on first-principles hybrid functional calculations, we demonstrate that not all co-doping approaches are beneficial for p-type doping. We show that the combination of one single donor + one double acceptor (e.g., $V_{Cd} + Cl_{Te}$) is usually most beneficial to the p-type doping due to the strong Coulomb binding between the donor-acceptor pairs, especially when the system contains enough Cd vacancies and the Cl treatment temperature is relatively low. The combination of two acceptors + one donor (e.g., $2Cu_{Cd} + Cl_{Te}$) helps very little in improving the shallowness of acceptor levels due to the coexistence of acceptor-acceptor and donor-acceptor coupling and will usually lead to an increase in defect formation energy because the energy cost of forming extra point defects is not adequately compensated by the Coulomb interaction between co-dopants. Co-doping one deep acceptor + one shallow acceptor (e.g., $P_{Te} + Sb_{Te}$) will produce an even deeper acceptor level because the deep acceptor is acting as a donor with its energy level pushed up by the shallow level. Our results, therefore, broaden the understanding of co-doping and provide a guideline for the future design of shallow defect complexes in CdTe, which can also be extended to other semiconductors.

ACKNOWLEDGMENTS

This paper was supported by the National Natural Science Foundation of China (Grants No. 11991060, No. 11634003, No. 12088101, and No. U1930402). We also acknowledge the computational support from the Beijing Computational Science Research Center.

[1] H. Katayama-Yoshida and T. Yamamoto, Materials design of the codoping for the fabrication of low-resistivity p-type ZnSe and GaN by *ab-initio* electronic structure calculation, Phys. Status Solidi B **202**, 763 (1997).

[2] H. Katayama-Yoshida, T. Nishimatsu, T. Yamamoto, and N. Orita, Codoping method for the fabrication of low-resistivity wide band-gap semiconductors in p-type GaN, p-type AlN and n-type diamond: prediction versus experiment, J. Phys.: Condens. Matter **13**, 8901 (2001).

[3] S. B. Zhang, S. H. Wei, and Y. Yan, The thermodynamics of codoping: how does it work?, Physica B **302** 135 (2001).

[4] J. Li, S.-H. Wei, S.-S. Li, and J.-B. Xia, Design of shallow acceptors in ZnO: first-principles band-structure calculations, Phys. Rev. B **74**, 081201 (2006).

[5] J. P. Chamonal, E. Molva, and J. L. Pautrat, Identification of Cu and Ag acceptors in CdTe, Solid State Commun. **43**, 801 (1982).

[6] J.-H. Yang, W.-J. Yin, J.-S. Park, W. Metzger, and S.-H. Wei, First-principles study of roles of Cu and Cl in polycrystalline CdTe, J. Appl. Phys. **119**, 045104 (2016).

[7] T. Okamoto, A. Yamada, and M. Konagai, Optical and electrical characterizations of highly efficient CdTe thin film solar cells, Thin Solid Films **387**, 6 (2001).

[8] V. Lyahovitskaya, L. Chernyak, J. Greenberg, L. Kaplan, and D. Cahen, n- and p-type post-growth self-doping of CdTe single crystals, J. Cryst. Growth **214–215**, 1155 (2000).

[9] J. J. Loferski, Theoretical considerations governing the choice of the optimum semiconductor for photovoltaic solar energy conversion, J. Appl. Phys. **27**, 777 (1956).

[10] M. Fiederle, V. Babentsov, J. Franc, A. Fauler, and J.-P. Konrath, Growth of high resistivity CdTe and (Cd,Zn)Te crystals, Cryst. Res. Technol. **38**, 588 (2003).

[11] Best Research-Cell Efficiency Chart; National Renewable Energy Laboratory, https://www.nrel.gov/pv/cell-efficiency.html (Accessed: September 2021).

[12] J. Ma, D. Kuciauskas, D. Albin, R. Bhattacharya, M. Reese, T. Barnes, J. V. Li, T. Gessert, and S.-H. Wei, Dependence of the Minority-Carrier Lifetime on the Stoichiometry of CdTe Using Time-Resolved Photoluminescence and First-Principles Calculations, Phys. Rev. Lett. **111**, 067402 (2013).

[13] M. O. Reese, C. L. Perkins, J. M. Burst, S. Farrell, T. M. Barnes, S. W. Johnston, D. Kuciauskas, T. A. Gessert, and W. K. Metzger, Intrinsic surface passivation of CdTe, J. Appl. Phys. **118**, 155305 (2015).

[14] J. H. Park, S. Farrell, R. Kodama, C. Blissett, X. Wang, E. Colegrove, W. K. Metzger, T. A. Gessert, and S. Sivananthan, Incorporation and activation of arsenic dopant in single-crystal CdTe grown on Si by molecular beam epitaxy, J. Electron. Mater. **43**, 2998 (2014).

[15] J. M. Burst, J. N. Duenow, D. S. Albin, E. Colegrove, M. O. Reese, J. A. Aguiar, C. S. Jiang, M. K. Patel, M. M. Al-Jassim, D. Kuciauskas, T. A. S. Swain, K. G. Lynn, and W. K. Metzger,

CdTe solar cells with open-circuit voltage breaking the 1 V barrier, Nat. Energy **1**, 16015 (2016).

[16] A. Nagaoka, D. Kuciauskas, J. McCoy, and M. A. Scarpulla, High *p*-type doping, mobility, and photocarrier lifetime in arsenic-doped CdTe single crystals, Appl. Phys. Lett. **112**, 192101 (2018).

[17] W. K. Metzger, S. Grover, D. Lu, E. Colegrove, J. Moseley, C. L. Perkins, X. Li, R. Mallick, W. Zhang, R. Malik, J. Kephart, C.-S. Jiang, D. Kuciauskas, D. S. Albin, M. M. Al-Jassim, G. Xiong, and M. Gloeckler, Exceeding 20% efficiency with *in situ* group V doping in polycrystalline CdTe solar cells, Nat. Energy **4**, 837 (2019).

[18] E. Colegrove, J. H. Yang, S. P. Harvey, M. R. Young, J. M. Burst, J. N. Duenow, D. S. Albin, S.-H. Wei, and W. K. Metzger, Experimental and theoretical comparison of Sb, As, and P diffusion mechanisms and doping in CdTe, J. Phys. D: Appl. Phys. **51**, 075102 (2018).

[19] B. Dou, Q. Sun, and S.-H. Wei, Optimization of Doping CdTe with Group-V Elements: A First-Principles Study, Phys. Rev. Applied **15**, 054045 (2021).

[20] E. Colegrove, S. P. Harvey, J. H. Yang, J. M. Burst, J. N. Duenow, D. S. Albin, S.-H. Wei, and W. K. Metzger, Antimony diffusion in CdTe, IEEE J. Photovolt. **7**, 870 (2017).

[21] S.-H. Wei and S. B. Zhang, Chemical trends of defect formation and doping limit in II-VI semiconductors: the case of CdTe, Phys. Rev. B **66**, 155211 (2002).

[22] W. Kohn and L. J. Sham, Self-consistent equations including exchange and correlation effects, Phys. Rev. **140**, A1133 (1965).

[23] G. Kresse and D. Joubert, From ultrasoft pseudopotentials to the projector augmented-wave method, Phys. Rev. B **59**, 1758 (1999).

[24] G. Kresse and J. Furthmüller, Efficient iterative schemes for *ab initio* total-energy calculations using a plane-wave basis set, Phys. Rev. B **54**, 11169 (1996).

[25] J. Paier, M. Marsman, K. Hummer, G. Kresse, I. C. Gerber, and J. G. Ángyán, Screened hybrid density functionals applied to solids, J. Chem. Phys. **124**, 154709 (2006).

[26] J. P. Perdew and M. Levy, Physical Content of the Exact Kohn-Sham Orbital Energies: Band Gaps and Derivative Discontinuities, Phys. Rev. Lett. **51**, 1884 (1983).

[27] G. Lutz, *Semiconductor Radiation Detectors. Device physics* (Springer, Berlin, 1999).

[28] S.-H. Wei, Overcoming the doping bottleneck in semiconductors, Comput. Mater. Sci. **30**, 337 (2004).

[29] W. Orellana, E. Menéndez-Proupin, and M. A. Flores, Self-compensation in chlorine-doped CdTe, Sci. Rep. **9**, 9194 (2019).

[30] D. R. Lide, *CRC Handbook of Chemistry and Physics* (CRC Press, New York, 2000), 81st edition.

[31] H. Zhu, M. Gu, L. Huang, J. Wang, and X. Wu, Structural and electronic properties of CdTe:Cl from first-principles, Mater. Chem. Phys. **143**, 637 (2014).

[32] A. Nagaoka, K. Nishioka, K. Yoshino, R. Katsube, Y. Nose, T. Masuda, and M. A. Scarpulla, Comparison of Sb, As, and P doping in Cd-rich CdTe single crystals: doping properties, persistent photoconductivity, and long-term stability, Appl. Phys. Lett. **116**, 132102 (2020).

[33] J. J. McCoy, S. K. Swain, J. R. Sieber, D. R. Diercks, B. P. Gorman, and K. G. Lynn, *p*-type doping efficiency in CdTe: influence of second phase formation, J. Appl. Phys. **123**, 161579 (2018).

[34] J.-H. Yang, J.-S. Park, J. Kang, W. Metzger, T. Barnes, and S.-H. Wei, Tuning the Fermi level beyond the equilibrium doping limit through quenching: the case of CdTe, Phys. Rev. B **90**, 245202 (2014).

[35] A. Lindström, M. Klintenberg, B. Sanyal, and S. Mirbt, Cl-doping of Te-rich CdTe: complex formation, self-compensation and self-purification from first principles, AIP Adv. **5**, 087101 (2015).

[36] D. M. Hofmann, P. Omling, H. G. Grimmeiss, B. K. Meyer, K. W. Benz, and D. Sinerius, Identification of the chlorine A center in CdTe, Phys. Rev. B **45**, 6247 (1992).

[37] A. Castaldini, A. Cavallini, B. Fraboni, P. Fernandez, and J. Piqueras, Comparison of electrical and luminescence data for the A center in CdTe, Appl. Phys. Lett. **69**, 3510 (1996).

[38] A. Castaldini, A. Cavallini, B. Fraboni, P. Fernandez, and J. Piqueras, Deep energy levels in CdTe and CdZnTe, J. Appl. Phys. **83**, 2121 (1998).

[39] K. Biswas and M.-H. Du, What causes high resistivity in CdTe, New J. Phys. **14**, 063020 (2012).